

AUTOMATIC MULTI-IMAGE PHOTO-TEXTURING OF 3D SURFACE MODELS OBTAINED WITH LASER SCANNING

L. Grammatikopoulos¹, I. Kalisperakis¹, G. Karras¹, T. Kokkinos¹, E. Petsa²

¹Laboratory of Photogrammetry, Department of Surveying,
National Technical University of Athens (NTUA), GR-15780 Athens, Greece
²Department of Surveying, The Technological Educational Institute of Athens (TEI-A),
Ag. Spyridonos Str., GR-12210 Athens, Greece

E-mail: lazaros@central.ntua.gr, ilias_k@central.ntua.gr, gkarras@central.ntua.gr, petsa@teiath.gr

KEY WORDS: Automation, Texture, Laser scanning, Orthorectification, DEM/DTM, Visualization, Heritage Conservation

ABSTRACT

The basic photogrammetric deliverable in heritage conservation is orthophotography (and other suitable raster projections) – closely followed today by a growing demand for photo-textured 3D surface models. The fundamental limitation of conventional photogrammetric software is twofold: it can handle neither fully 3D surface descriptions nor the question of image visibility. As a consequence, software which ignores both surface and image occlusions is clearly inadequate for the complex surface topography encountered, as a rule, in conservation or restoration tasks; geometric accuracy and good visual quality are then possible only at the cost of tiresome human interaction, especially in the phase of surface modeling. However, laser scanning and powerful modeling/editing software allow today fast and accurate collection of vast numbers of surface points and the creation of reliable 3D meshes. Close-range photogrammetry is obviously expected to extend its horizon by taking full advantage of this new possibility.

Here an approach is presented for the automated generation of orthoimages and perspective views from fully 3D surface descriptions derived from laser scanning. Initially, the algorithm detects surface occlusions for the novel view. Next – in contrast to conventional photogrammetric software which requires an operator to define individual original images as the source for image content – all available images participate in a view-independent texturing of the new image. Thus, following a bundle adjustment, all surface triangles are back-projected onto all initial images to establish visibilities. Texture “blending” is realised via an appropriate weighting scheme, which regulates the local radiometric contribution of each original image involved. Finally, a basic statistical test allows to automatically filter out outlying colour values. At its present stage of implementation, the algorithm has been tried at the example of a Byzantine church in Athens. It is concluded that the presented combination of laser scanning with photogrammetry – resulting in geometric accuracy, high visual quality and speed – is essentially capable to automatically create novel views from several images, and hence provide a realistic, practicable approach in heritage conservation. Finally, several elaborations of the approach are also suggested.

1. INTRODUCTION

Thanks to the combination of geometric accuracy with textured representation, the digital orthomosaics rank high among photogrammetric products for the documentation of cultural heritage. Obviously, this is not meant to underrate other related products (raster developments, cartographic projections, drapings, photo-realism, animation). In fact, digital orthorectification exemplifies here a core task of photogrammetry, namely the combination of surface modeling and photo-texturing.

Mavromati et al. (2002) outline a series of problems peculiar to orthoimaging of cultural items (the use of off-the-shelf cameras on unstable platforms, related difficulties in controlling imaging geometry and, hence, in performing the bundle adjustment etc.). Yet, accurate surface modeling remains a matter of primary importance. And it is stressed that 3D models are not simply prerequisites for projection or rendering. Although when only photo-realistic visualizations are required image-based rendering tools may provide a direct answer (Beraldin et al., 2002), photogrammetry typically relies on model-based texturing, as it is mostly asked to also offer explicit 3D data and representations, to facilitate geometric or morphological documentation and analysis.

Close-range applications are usually faced with complex object shapes – a fact raising significant occlusion problems. In this sense, surface modeling is the key factor if textured representations both geometrically reliable and visually correct (free from ‘melting’ or ‘stretching’) are expected. Conventionally, surface

points are collected with stereoscopic viewing in digital photogrammetric workstations (commercial matching software is generally unsuitable for archaeological objects, needing considerable editing). Even so, an appropriate strategy for breakline and point measurement can indeed produce results of high quality – provided that effort and time are not an issue (Mavromati et al., 2003). Further limitations include registration problems among stereopair-based 3D models for images taken all around the object. Yet, at the other extreme of image-based modeling, powerful approaches are being developed – in the field of computer vision – for the automatic extraction of 3D surface models from image sequences with no prior information about camera or object. Although models of high visual quality are thus produced, it appears that the obtained accuracies are not yet in position to meet the requirements for most mapping applications (Pollefeys et al., 2000). The actual metric potential of advanced techniques for automatic dense reconstruction employing a limited number of multiple wide-baseline images (Strecha et al., 2003) also remains to be further assessed.

Today, range-based modeling through laser scanning represents a powerful technology, capable of sampling enormous numbers of surface points at very fast rates; therefore, it may provide the required 3D support for orthorectification. In a wider sense, the same is also true for generating photo-textured virtual models of real-world scenes, notably in the computer graphics field, where visual quality indeed represents a major concern (Bernardini et al., 2001; Corrêa et al., 2002). As put by Beraldin et al. (2002), high-resolution recording of cultural sites, and the possibility to

promote them through virtual 3D visits, stimulate research, particularly as regards fusion of laser scanning and colour imagery. Some commercial 3D systems provide model-registered colour texture, but limited image quality generally makes the acquisition of separate images with higher resolution necessary. This is clearly true also for the high requirements of orthoimaging.

Of course, laser scanning approaches are also faced with certain problems – besides the high cost. Thus, post-processing of large volumes of raw data for mesh triangulation (including noise removal and hole-filling) is, indeed, a quite demanding procedure (Böhler et al., 2003). But important in the present context is that common orthoprojection software may only handle surfaces described as DTMs with a unique elevation at each planimetric XY location. Thus, all scanned 3D points are typically processed by 2D triangulation into a 2.5D mesh – which has predictable consequences on the final orthoimage (Mavromati et al., 2003, give such an example). Inevitably, orthoimaging algorithms for fully 3D models need to be introduced.

Such algorithms have primarily to handle the question of visibility – in order to avoid the common flaws of orthoimaging (displacement, blind areas, double-projection) – which is twofold:

- First, it must be established which individual surface units or ‘groundels’ are actually visible in the desired direction of (ortho)projection. Outcome of this step is that to each orthoimage pixel a unique elevation is assigned.
- Next, one has to check which surface points, among those established above for a particular projection, are also visible from the perspective centre of the input image used. In case of occlusion, colour value can be extracted from an adjacent image.

Such methods, relying on dense regular DTMs derived via laser scanning, have been reported in both aerial and terrestrial cases (Kim et al., 2000; Boccardo et al., 2001). Following a standard photogrammetric practice, texture for visible surface patches is extracted here from one corresponding original image. If more overlapping images are at hand, the source image can be selected according to different possible criteria (imaging distance or angle formed by the projective ray and the surface; size of the imaged surface triangle).

Yet, this ‘single-image’ texturing approach may well lead to adjacent surface triangles receiving colour from different images with varying radiometric characteristics, which may lead to discontinuity artifacts and radiometric distortion at triangle borders (El-Hakim et al., 2003). Colour interpolation (‘blending’) is the response to this. For every point, appropriately weighted combinations of corresponding triangle textures from all images, or an image subset, are used (Neugebauer & Klein, 1999; Bernardini et al., 2001; Buehler et al., 2001; Wang et al., 2001; Rocchini et al., 2002). Such a smoothing of radiometric difference produces seamless texture free from jumps in colour appearance – at the possible cost of a certain blurring effect (El-Hakim et al., 2003). These approaches have been developed in the field of computer graphics, where life-like animations, realism or illumination are evidently crucial issues. Hence, a weighting strategy is formulated mostly in the context of ‘view-dependent’ texture mapping, in which interpolation schemes favour images seeing the object or scene closest in angle to the current viewing direction. In this way, surface specularities or incorrect model geometry may be better captured (Debevec et al., 1996, 1998).

However, Wang et al. (2001) have pointed out that the use of a single texture map for a 3D model is usually sufficient. In this sense, it seems that static, rather than dynamic, texturing is preferable (being somehow more ‘objective’) for most instances of photogrammetric mapping. Thus, a view-independent algorithm

weights the contribution of participating input images according to their spatial relation to the object surface (e.g. distance, angle of view) and their characteristics (camera constant, resolution) in order to assign a unique colour value to each individual surface unit (Poulin et al., 1998; see also Grün et al., 2001).

To a certain extent, colour blending is at the same time an ‘error filtering’ process; yet, existing error sources can still cause geometric and radiometric distortions. To start with, a final product is inevitably affected by the accuracy of image orientations and camera calibration; a bundle adjustment with self-calibration – incorporating lens distortion – is indispensable. The accuracy of 3D recording, the quality of surface description by 3D faces and model registration are further possible reasons for texture misalignments. Blurring due to significant differences in resolution of the source images has also been noted in this context (Neugebauer & Klein, 1999; Buehler et al., 2001). This latter problem, however, is rather uncommon in photogrammetric applications.

In this contribution, an approach is presented for automatically generating orthoimages and perspective views from a 3D mesh, obtained via laser scanning. Briefly put, the implemented algorithm: identifies all surface triangles seen in the particular projection; next, it establishes which of them appear on each available image; the pixels of the novel image are then coloured by weighted blending of texture from all viewing images; outlying colour data are automatically excluded. Results of experimental applications will also be given.

2. VISIBILITY CHECK AND TEXTURE BLENDING

For this procedure, the following input data are required:

- a triangulated 3D mesh in the form of successive XYZ triplets describing the object surface;
- grayscale or colour images along with their interior and exterior orientation parameters;
- the equation in space of the projection plane;
- the endpoints in object space, if necessary, of the area to be projected;
- the pixel size of the new digital image.

It is seen that, besides orthogonal, oblique projections may also be accommodated.

The initial fundamental task is to handle the occlusion problem, namely: a) to establish model areas which are not visible on the novel image; b) to establish model areas not seen on a particular image. In this way, one also: c) establishes image areas which must not appear in the novel image; d) establishes visible model areas to which the particular image has no texture to contribute. This is illustrated in Fig. 1.

2.1 Model occlusions

First, the question of surface visibility in the desired direction is addressed. To this end, the triangulated 3D mesh is orthogonally projected onto the specified projection plane. To speed up the search process, the orthoimage area is tessellated into a rectangular grid with cells larger than those of the orthoimage, e.g. by 5 times (the size depends on factors such as available computer memory, model size and size of the new image). For each (projected) 2D triangle, its circumscribing orthogonal parallelogram is formed, occupying a number of adjacent grid cells, to which the identity number (ID) of the particular triangle is assigned.

This is repeated for all triangles, resulting into a table containing all triangle IDs ascribed to each individual grid cell. All projected triangles containing a particular pixel of the orthoimage

may be, thus, established by checking only a limited number of triangles, namely those ascribed to the corresponding grid cell. Among these model triangles which are intersected in space by the projection line of a particular orthoimage pixel, that whose intersection yields the largest elevation value is kept; this value – which provides the Z-value of the orthoimage pixel – is stored along with the triangle ID number. In this fashion, the question of model visibility/occlusion has been handled.

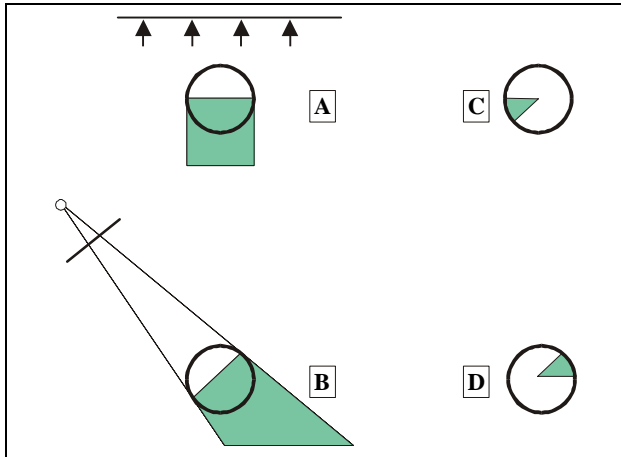


Figure 1. The visibility question. A: area occluded in the projection; B: area occluded on the image; C: imaged area not seen on the projection; D: model area with no available texture.

2.2 Image occlusions

Addressing now the second visibility issue, all 3D triangles are centrally projected, through the available orientation/calibration data, onto all images involved. For all planimetric XY values of the orthoimage and their assigned Z-value, corresponding image coordinates xy on all images are calculated. Adopting a similar search scheme, as before, among all model triangles intersected by a particular image ray the one closer to the projective center is the triangle actually recorded on the image. If its ID number does not coincide with the one already ascribed at the preceding stage to the orthoimage pixel, it is established that the surface point corresponding to this particular ortho pixel is occluded on the examined image. If, on the contrary, the two triangle IDs are identical, then the model point is indeed visible on the studied image, and the RGB values are stored.

Despite the computational burden, colour values are interpolated in the present implementation by bicubic convolution, since it provides an obviously smoother result. However, it is evident that adjacent pixels do not necessarily relate to adjacent model points. Although no discernible effects emerged in the applications, checks may possibly be considered to omit such pixels.

2.3 Colour interpolation

Outcome of the previous step for all orthoimage pixels is colour values from several images – unless the particular surface point is invisible on all images (such orthoimage pixels are marked as undefined by a specific colour value). For these regions, ‘hole-filling’ tools may extract colour values from surrounding model regions (Debevec et al., 1998; Poulin et al., 1998), a possibility not examined here. The algorithm, however, can generate a map with the distribution of orthoimage areas which are visible on 0, 1, 2 and > 2 source images (cf. Fig. 9 below). Hence, additional images, if available, may eventually be introduced into the process to fill the gaps. Besides, it is useful to know which ortho-

image areas are visible on more than 2 images, as this allows a test to detect and exclude outliers.

Indeed, in order to assign a final colour value to the orthoimage pixels, outlying values must be excluded. Besides model faults, these can generally also originate from view-dependent features – obstacles, specular highlights, transparencies, mirrors, refractions etc. (Poulin et al., 1998; Rocchini et al., 2001). Yet, higher significance in photogrammetry has probably the case when one approaches surface regions invisible to a camera, i. e. occlusion borders (Neugebauer & Klein, 1999; Buehler et al., 2001). This may cause the emergence of artifacts, as even small orientation and registration (or modeling) errors could lead to colour erroneously derived from an occluding or, respectively, an occluded model point (Fig. 2 shows such an example; see Fig. 7, but also Fig. 6). One may possibly evaluate the ‘occlusion risk’ of pixels – for instance, by checking the imaging distance against that of neighbouring pixels from their own visible model point. This is a topic of future study.

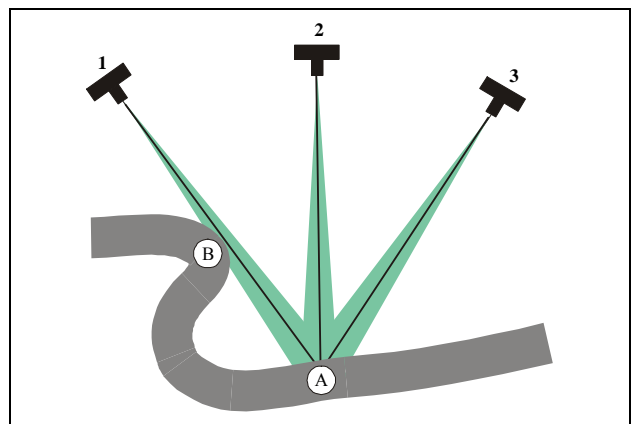


Figure 2. Due to small modeling, calibration and orientation errors, the texture of point B on image 1 may be assigned to A.

At this stage, a basic statistical test has been adopted, provided that sufficient (> 2) colour values are available for a particular orthoimage pixel. Mean (μ) and standard deviation (σ) of colour values are computed each time; individual colour values falling outside the range $\mu \pm \beta \times \sigma$ are excluded. It is estimated that the value of factor β could be around 1 (in the test presented in the next section using seven images, β was set to 1).

Subsequently, the valid contributing colour values from all participating images are used to generate the final texture of every orthoimage pixel, which is calculated as a weighted mean of all contributing images. In view-independent texture mapping, the main factors influencing colour quality are scale (i. e. imaging distance and camera constant) of the source image; its viewing angle (i. e. the angle formed by the intersection of the image ray and the model triangle); and image resolution. These factors are in fact all combined to yield the size (in pixels) of the 2D triangle on each image, which is regarded as a reliable indication for the ‘strength’ of the extracted colour. Thus, as suggested by Poulin et al. (1998) and illustrated in Fig. 3, the contribution of all participating colour values are weighted as relative functions of the corresponding 2D image triangle surface areas (a weighting scheme also adopted by Grün et al., 2001).

Initially, the algorithm has been developed in MatLab and then implemented in C. In order to verify its performance, but also increase speed, tests were first performed employing synthetic images, with error-free orientations, generated from an existing photo-textured 3D building model (Kokkinos, 2004).

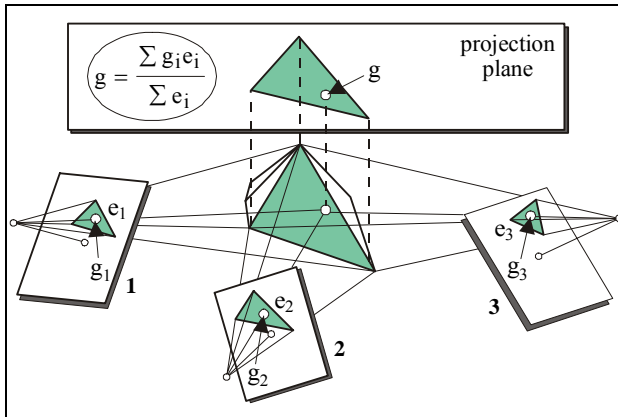


Figure 3. Each image contributes a colour value g according to the surface area e of the image triangle containing the point.

3. PRACTICAL EVALUATION

The object of the experimental application was the entrance of the 11th century church of ‘Kapnikarea’, an important Byzantine monument in the centre of Athens. Mainly due to its columns, the object is sufficiently complex for the task.

3.1 Surface scanning and modeling

For surface recording, the Mensi GS200 laser scanner was used. This device scans at a rate of 5000 points/sec, having a 60° vertical field of view. Three separate scans were carried out from a distance of about 5 m, for which a typical value ± 1.4 mm of the standard deviation is given (the resolution is 4 mm at a distance of 10 m). For registration, 6 well distributed target spheres were employed, also measured geodetically. The software *RealWorks Survey 4.1.2* was used for the target-based registration of scans. The precision of geo-referencing was about ± 2.5 mm. A total of 7 million surface points were obtained. These were edited using the *Geomagic Studio* software, and were subsequently reduced to 1 million points to provide a final 3D mesh, which consisted of 3 million triangles (a view is seen in Fig. 4).

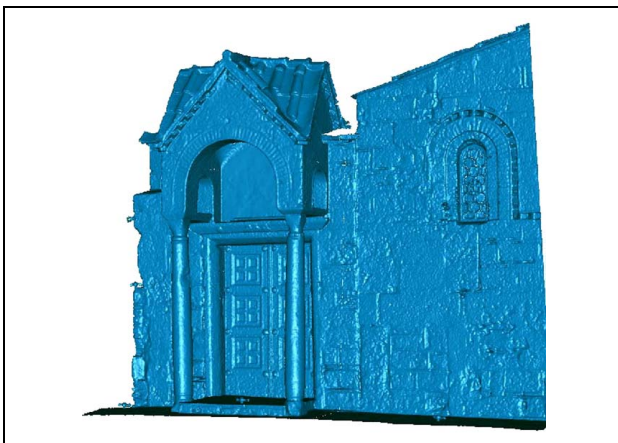


Figure 4. View of the full 3D model

3.2 Bundle adjustment

The object has been recorded with different analogue and digital cameras, to be used in future tests. Here, results are given for images from a Sony 5 MegaPixel camera (2592×1944). A total of 7 images were selected, taken with fixed focusing to keep interior orientation invariant. All images used are seen in Fig. 5.

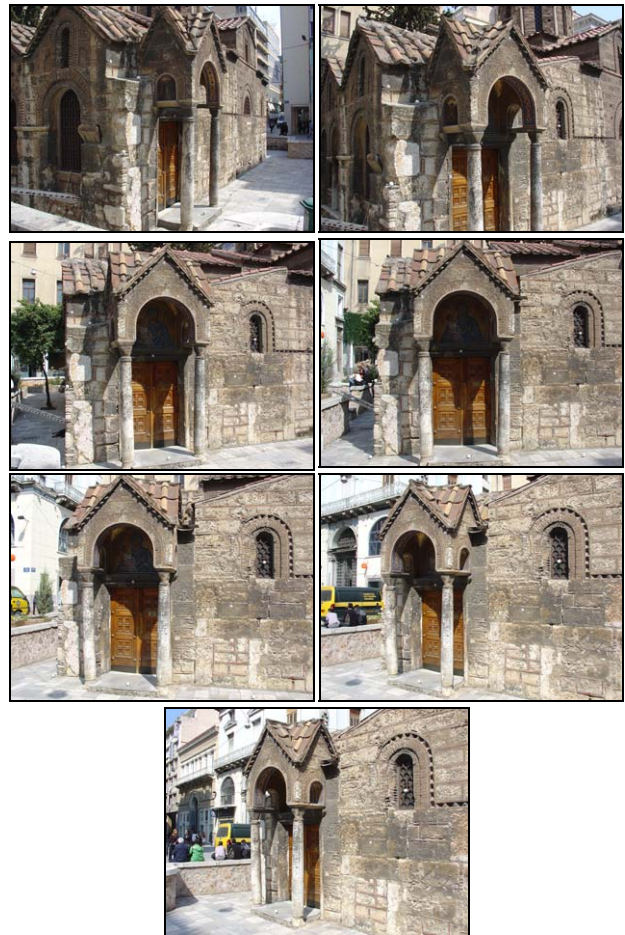


Figure 5. The seven images used in the project.

Based on 18 signalled object control points (most of them seen on all images) and using our own software *Basta*, bundle adjustment with self-calibration (including coefficients k_1 , k_2 of radial symmetric lens distortion) was carried out using 8 tie points. It was possible to achieve a high accuracy, as seen in Table 1. The significance of the radial distortion effect is clear in the results; a practical test (see below) has indeed illustrated why it cannot be ignored – at least in multi-image texturing methods.

σ_0 (pixel)	± 0.28	± 2.40
c (pixel)	2573.94 ± 1.36	2509.35 ± 9.42
x_0 (pixel)	10.27 ± 1.03	-16.67 ± 8.47
y_0 (pixel)	7.35 ± 0.87	-33.46 ± 6.80
k_1 ($\times 10^8$)	-2.98 ± 0.04	
k_2 ($\times 10^{15}$)	4.90 ± 0.19	
rms (GCP)	0.3 mm	1.8 mm
σ (tie points)	1.3 mm	8.0 mm

Using these camera calibration and exterior orientation data, the images were then used to colour the projections of the model.

3.3 Generation of photo-textured projections

All images used here had been acquired successively (under the same lighting conditions); thus, since no radiometric variations among images were observed, texture averaging was considered as adequate (for pre-processing see e. g. Grün et al., 2001). The

plane of the church façade was selected as projection plane. The orthoimage pixel size was set to 2 mm. As mentioned, the algorithm establishes image visibility/occlusion for all surface parts which have been previously identified as visible in the direction of projection. Results for an individual image are seen in Fig. 6.

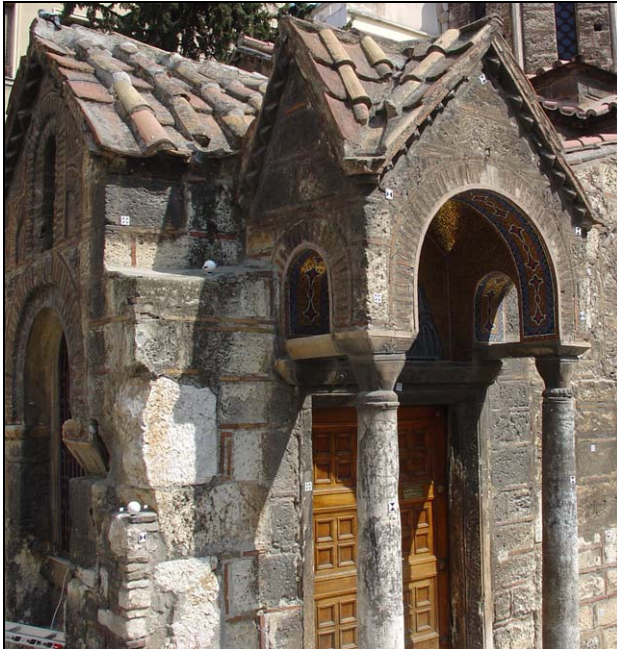


Figure 6. Orthoprojection (below) of the image above. At the right silhouettes of the columns texturing problems are seen.

The problem of outlying colour values (also observed in Fig. 6), particularly in the vicinity of occlusion borders (cf. section 2.3 and Fig. 2) is illustrated in Fig. 7: above, an extract is shown of

the orthoimage derived from all source images without blunder-filtering. The white artifact – which clearly originates from the occlusion border of the image in the middle – vanishes if colour values deviating more than $\pm\sigma$ from the mean are automatically ignored (below).

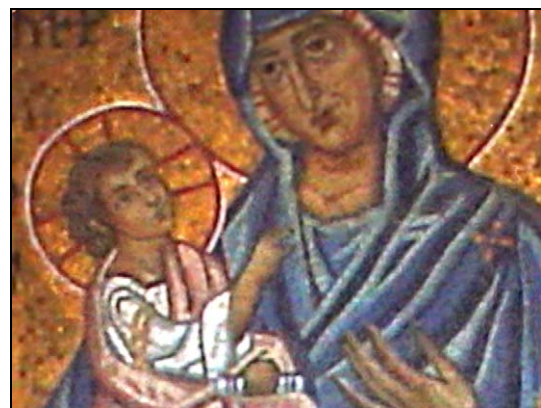


Figure 7. Part of the orthoimage from 7 images without (above) and with (below) outlier filtering. In the middle is the source image which causes the artifact with its occlusion border.

The final orthoprojection, automatically generated with the contribution of all 7 images, seen in Fig. 5, is presented in the left of Fig. 8. The result is essentially satisfactory. The main imperfections are small holes due to lack of texture (the camera had not been elevated). Other flaws – for instance, some aliasing at certain edges which, however, may not be perfectly perpendicular to the projection plane – are observed only with considerable zooming.

On the right of Fig. 8, a vertical section is presented utilising all available model and texture information, including parts which are not visible on the left (e. g. a part of the arches).



Figure 8. Left: Extract of the orthoimage from 7 images. Right: orthoprojection of a model section defined by a maximum Z-value.

Regarding speed, a PC (CPU Athlon XP 2.4 GHz, 512 MB RAM) required 5 min to project 3 million triangles onto the images, in a suitable order to facilitate the last step; 1 min to establish the Z-values for each orthoimage pixel; 13 minutes for the production of a final 3720×2775 image from seven 2592×1944 images.

Filtering out of colour value outliers not only helps to avoid the emergence of artifacts, it also produces much sharper images. In the present example, this was feasible since practically the total model area was visible on three and more images (see Fig. 9).

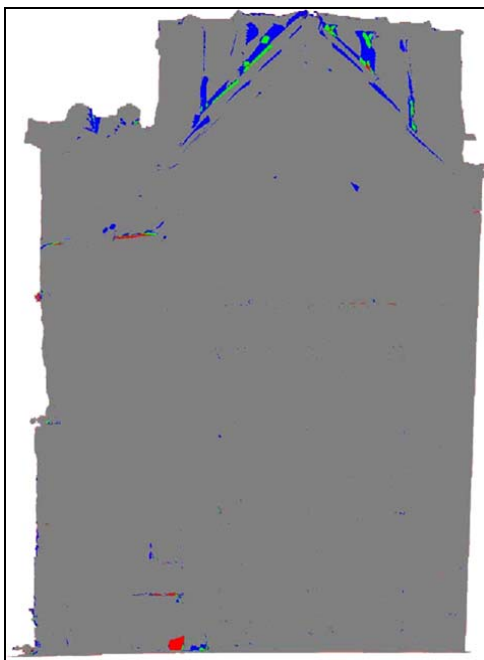


Figure 9. Map of surface coverage: areas seen in 0 image (red), 1 image (green), 2 images (blue) and > 2 images (grey).



Figure 10. Corresponding orthoimages patches, from 7 images, without (above) and with (below) correction of lens distortion.

On the other hand, as already mentioned, uncorrected lens distortion is also a source of severe blurring. In Fig. 10, the effects of uncorrected lens distortion are seen in the neighbourhood of signalled control points. Here, the simple exclusion of outliers

has obviously nothing significant to offer; the incorporation of additional parameters in the bundle adjustment is indispensable.



Figure 11. Original image (above) and synthetic perspective view with the same 'camera' and orientation.

Finally, the presented algorithm is also in position to create perspective views, required in several cases (but also used for the generation of photorealistic animations). In this instance, novel views are central projections of the surface, using freely chosen values for the calibration/orientation parameters of the fictitious camera. This is illustrated in Fig. 11, which depicts an original image along with a synthetic one, generated from the remaining 6 images using the exact orientation data of the initial image.

4. CONCLUDING REMARKS

An algorithm has been implemented for the automatic synthesis of textured views, given a 3D triangulated mesh and precise calibration/orientation data for several overlapping images. Model and image visibility are identified, to allow pixel colouring with the weighted average from all viewing images, whereby a basic blunder detection tool allows to avoid artifacts. The product for the particular object studied here is indeed very satisfactory.

Yet, further enhancements of the technique are both necessary and feasible (Grammatikopoulos et al., 2004). Thus, some hole-

filling tools should be introduced. Besides, more robust means for outlier avoidance must be experimented with. For example, closeness of a source pixel to an occlusion border may be taken into account. Further, image matching has been used for model and registration refinement (Debevec et al., 1996; also Bernardini et al., 2001). Indeed, a multiple image coverage and precise starting values supplied by the 3D surface model may allow to refine the model and/or the textured output. The above remarks indicate possible future tasks of the work presented here.

Acknowledgements

The authors sincerely thank Drs. V. Balis and C. Liapakis of GEO-TECH Ltd. (representative of Trimble in Greece) for providing the scans and ground control. We are also grateful to INFOCAD Ltd. (representative of Geomagic Studio in Greece) for kindly providing the license to use this software.

REFERENCES

- Beraldin J.-A., Picard, M., El-Hakim, S. F., Godin, G., Latouche, C., Valzano, V., Bandiera, A., 2002. Exploring a Byzantine crypt through a high-resolution texture mapped 3D model: combining range data and photogrammetry. Proc. CIPA Int. Workshop on Scanning for Cultural Heritage Recoding, pp. 65-70.
- Bernardini, F., Martin, I. M., Rushmeier, H., 2001. High-quality texture reconstruction from multiple scans. IEEE Trans. Visualization & Computer Graphics, 7(4):318-332.
- Boccardo, P., Dequal, S., Lingua, A., Rinaudo, F., 2001. True digital orthophoto for architectural and archaeological applications. Proc. Int. Workshop on Recreating the Past: Visualization & Animation of Cultural Heritage, Ayuttaya, Thailand (in CD).
- Böhler, W., Bordas Vicent, M., Hanke, K., Marbs, A., 2003. Documentation of German Emperor Maximilian I's tomb. Proc. XIX CIPA Int. Symposium, Antalya, Turkey, pp. 474-479.
- Buehler, C., Bosse, M., McMillan, L., Gortler, S., Cohen, M., 2001. Unstructured lumigraph rendering. Proc. ACM SIGGRAPH Annual Conference Series, pp. 425-432.
- Corrêa, W., Oliveira, M., Silva, C., Wang, J., 2002. Modeling and rendering of real environments. RITA, IX(1), pp. 1-32.
- Debevec, P., Taylor, C.J., Malik, G., 1996. Modeling and rendering architecture from photographs: a hybrid geometry- and image-based approach. ACM SIGGRAPH, pp. 11-20.
- Debevec P., Borshukov G., Yu Y., 1998. Efficient view-dependent image-based rendering with projective texture-mapping. Proc. 9th Eurographics Rendering Workshop, Rendering Techniques '98, Springer, pp. 14-26.
- El-Hakim, S., Gonzo, L., Picard, M., Girardi, S., Simoni, A., 2003. Visualization of frescoed surfaces: Buonconsiglio Castle – Aquila Tower, 'Cycle of the Months'. Int. Workshop on Visualization & Animation of Reality-Based 3D Models (in CD).
- Grammatikopoulos, L., Kalisperakis, I., Karras, G., Kokkinos, T., Petsa, E., 2004. On automatic orthoprojection and texture-mapping of 3D surface models. Int. Arch. Phot. & Rem. Sens, 35(5), pp. 360-365.
- Grün, A., Zhang, L., Visnovcova, J., 2001. Automatic reconstruction and visualization of a complex Buddha Tower of Bayon, Angkor, Cambodia. Proc. 21. Wissenschaftlich-Technische Jahrestagung der DGPF, pp. 289-301.

Kim, Y.-I., Kwon, O.-H., Kim, H.-T., 2000. Detecting and restoring the occlusion area for generating a digital orthoimage. Proc. ASPRS Annual Conference (in CD).

Kokkinos, T., 2004. Automatic Photo-Texturing of Projections of 3D Models. Diploma Thesis, Dept. of Surveying, NTUA.

Mavromati, D., Petsa, E., Karras, G., 2002. Theoretical and practical aspects of archaeological orthoimaging. *Int. Arch. Phot. & Rem. Sens.*, 34(B5), pp. 413-418.

Mavromati, D., Petsa, E., Karras, G., 2003. Experiences in photogrammetric archaeological recording. Proc. XIX CIPA Int. Symposium, Antalya, Turkey, pp. 666-669.

Neugebauer, P., Klein, K., 1999. Texturing 3D models of real world objects from multiple unregistered photographs views, Proc. Eurographics '99, Computer Graphics Forum, 18(3).

Pollefeys, M., Koch, R., Vergauwen, M., van Gool, L., 2000. Automated reconstruction of 3D scenes from sequences of images. *ISPRS J. Phot. & Rem. Sens.*, 55:251-267.

Poulin, P., Ouimet, M., Frasson, M.-C., 1998. Interactively modeling with photogrammetry. Proc. Eurographics Workshop on Rendering '98, pp. 93-104.

Rocchini, C., Cignoni, P., Montani, C., Scopigno, R., 2002. Acquiring, stitching and blending diffuse appearance attributes on 3D models. *The Visual Computer*, 18:186-204.

Strecha, C., Tuytelaars, T., van Gool, L., 2003. Dense matching of multiple wide-baseline views. Proc. 9th Int. Conf. on Computer Vision, ICCV '03, Vol. 2, pp. 1994-1201.

Wang, L., Kang, S.B., Szeliski, R., Shum, H.-Y., 2001. Optimal texture map reconstruction from multiple views, Proc. Computer Vision & Pattern Recognition, CVPR '01, vol. 1.